Liquid Crystal Polarization Camera

Lawrence B. Wolff, Todd A. Mancini, Philippe Pouliquen, and Andreas G. Andreou

***Abstract*— We present a fully automated system which unites CCD camera technology with liquid crystal technology to create a *polarization camera* capable of sensing the partial linear polarization of reflected light from objects at pixel resolution. As polarization sensing not only measures intensity but also additional physical parameters of light, it can therefore provide a richer set of descriptive physical constraints for the understanding of images. Recently it has been shown that polarization cues can be used to perform dielectric/metal material identification, specular and diffuse reflection component analysis, as well as complex image segmentations that would be significantly more complicated or even infeasible using intensity and color alone. Such analysis has so far been done with a linear polarizer mechanically rotated in front of a CCD camera. The full automation of resolving polarization components using liquid crystals not only affords an elegant application, but significantly speeds up the sensing of polarization components and reduces the amount of optical distortion present in the wobbling of a mechanically rotating polarizer. In our system two twisted nematic liquid crystals are placed in front of a fixed linear polarizer placed in front of a CCD camera. The application of a series of electrical pulses to the liquid crystals in synchronization with the CCD camera video frame rate produces a controlled sequence of polarization component images that are stored and processed on Datacube boards. We present a scheme for mapping a partial linear polarization state measured at a pixel into hue, saturation and intensity producing a representation for a partial linear polarization image. Our polarization camera currently senses partial linear polarization and outputs such a color representation image at 5 Hz. The unique vision understanding capabilities of our polarization camera system are demonstrated with experimental results showing polarization-based dielectric/metal material classification, specular reflection and occluding contour segmentations in a fairly complex scene, and surface orientation constraints.**

I. Introduction

AS HUMAN BEINGS we naturally think of vision in terms of perception of intensity and color. Polarization of light might appear to be of little relevance or benefit to automated vision systems simply because the human visual system is almost completely oblivious to this property of light. In fact the use of the polarization of light for automated vision systems is an augmentation of sensed light parameters from a scene of which intensity[1] of light is just one of these parameters. Polarization parameters being physically orthogonal to wavelength (i.e., color) and a more general set of physical parameters than intensity can carry additional information and therefore provide a richer description of an imaged scene. Because the study of polarization vision is more general than intensity vision there are polarization cues that can significantly simplify some important visual tasks which are more complicated or possibly infeasible when limited to using intensity and color information. This was shown to be true for tasks such as dielectric/metal discrimination in images [24], [25], segmentation of specularities [23], [27], [25], quantitative separation of specular and diffuse reflection components [23], [27], [25], and, direct identification of occluding contours [27], [4], [25]. Work has also been done on polarization based determination of shape [15], [22], [16].

Commercially available CCD camera sensors are geared toward taking intensity images, not for measuring polarization images. A practical difficulty in implementing automated polarization vision has been obtaining polarization component images using a linear polarizing filter in front of an intensity CCD camera and mechanically rotating this filter by hand or by motor into different orientations. To recover a reflected polarization image, multiple images of the same scene are required for different orientations of the linear polarizing filter. Not only can there be considerable time lag between rotating the polarizer into different orientations to achieve measurement of a single polarization image, but the mechanical process of rotating the filter itself introduces significant shifts in perspective projection of the scene onto the image plane, producing large reflected polarization measurement errors particularly at intensity discontinuities in the scene. There can be considerable advantages to building a camera sensor geared toward doing polarization vision, capable of taking polarization images without external mechanical manipulation of a filter. We call such a camera sensor a "polarization camera." There already exist polarization-based vision methods that may significantly benefit a number of potential application areas including aerial reconnaissance, autonomous navigation, inspection, and, manufacturing and quality control. A polarization camera would make polarization-based vision methods more accessible to these application areas and others. It should be fully realized that as intensity is a subset of polarization information, that a polarization camera can function as a conventional intensity camera, so that intensity vision methods can be implemented by such a camera either alone, or, together

Manuscript received October 1992; revised October 31, 1994. This work was supported in part by ARPA Contract F30602-92-C-0191, AFOSR Grant F49620-93-1-0484, and an NSF National Young Investigator Award IRI-9357757. This paper was recommended for publication by Associate Editor R. Howe and Editor R. A. Volz upon evaluation of the reviewers' comments.

L. B. Wolff and T. A. Mancini are with the Computer Vision Laboratory, Department of Computer Science, The Johns Hopkins University, Baltimore, MD 21218 USA.

P. Pouliquen and A. G. Andreou are with the Department of Electrical and Computer Engineering, The Johns Hopkins University, Baltimore, MD 21218 USA.

Publisher Item Identifier S 1042-296X(97)01046-X.

[1]The term "intensity" of light in this paper refers to the reflected radiance of light as precisely defined in [13]. As discussed in [13], image intensity precisely means image irradiance which is directly proportional to reflected light radiance.

with polarization-based vision methods. A camera sensor geared toward polarization vision does not in any way exclude intensity vision—it augments intensity vision providing more general physical input to an automated vision system.

Adding color sensing capability to a polarization camera makes it possible to measure states of partial linear polarization over multiple separate wavelength ranges which adds even more information. In this paper the implementation of a liquid crystal polarization camera utilizes a monochrome CCD camera photosensing light over the broadband range 400–700 NM. The measured partial linear polarization at a pixel is the weighted average of partial linear polarizations according to the spectral content of the reflected light and the photosensing response of the CCD camera.

We discuss and demonstrate in this paper particular implementations of two different aspects for the design of a polarization camera. The first is obviating the need for mechanically rotating a polarizing filter in front of an intensity camera sensor by using twisted nematic (TN) liquid crystals that electrooptically "steer" the plane of polarization of light. These kinds of liquid crystals are more typically used for producing graphical displays such as in laptop personal computers. We propose to apply the same physical principles of liquid crystal technology, but in a different way, to the measurement of *partial linearly polarized* light which consists of the sum of unpolarized and completely linearly polarized states. By electrically switching the states of TN liquid crystals in front of a fixed linear polarizer, measuring the components of partial linear polarization of reflected light from objects can be placed under full computer control. Whereas before the polarizer had to mechanically rotate relative to the plane of polarization of light to resolve components, the polarizer now remains fixed while instead it is the plane of polarization that is rotated by the liquid crystals. Currently this enables the automatic rapid sensing of 15 polarization component images per second, and eliminates optical distortion caused by a rotating polarizing filter particularly near high contrast intensity edges where even small subpixel shifts can produce a false measurement of high partial polarization. Altogether three unique components of polarization are sensed every 1/5 second to produce a complete partial linear polarization image.

The second aspect of a polarization camera that is addressed in this paper is the implementation of a natural visual representation for the polarization state of light at each pixel in a polarization image. How can humans be made to "see" reflected polarization, a phenomenon that nobody has ever directly observed except with the aid of special filters? This representation for polarization images should of course be amenable to quick computational processing by existing polarization-based algorithms that extract visual constraints from polarization information. It turns out that practically all light that is reflected and scattered in most environments [20] is partial linearly polarized. In the mid-1970's Bernard and Wehner [1] proposed a functional similarity between color and partial linear polarization perception in biological vision systems. Motivated by this we propose a scheme for representing partial linear polarization in an image. A state of partial linear polarization is uniquely mapped into hue-saturation-intensity color space where intensity maps into itself, and the two additional physical parameters of partial linear polarization that humans do not perceive are represented as the saturation of a color hue. This distinctly demonstrates how a partial linear polarization image is a generalization of a gray level intensity image. A number of polarization images taken with our liquid crystal polarization camera are demonstrated.

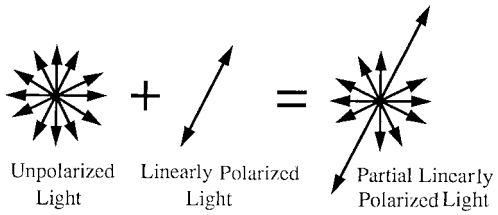

Fig. 1. An electric field distribution for partial linearly polarized light viewed head-on.

While physics is our primary motivation for studying polarization vision and building polarization cameras, it is important to note that there are a large number of biological visual systems within a variety of insects [17], [18], and fish [7], [10], that primarily rely on polarization sensing. Not only is polarization vision in biological systems probably historically older than human vision, but in sheer number, there are more natural polarization vision systems existing today than there are humans.

II. Brief Polarization Background

Fig. 1 shows an electric field distribution of partial linearly polarized light viewed head-on. This distribution is the superposition of an *unpolarized* component consisting of an isotropic electric field distribution, with a *linear polarized* component consisting of an electric field oriented along a single axis. Humans visually perceive the energy flux of this distribution as "intensity". What is not visually perceived are the relative magnitudes of unpolarized and linear polarized components that constitute the light, nor the orientation of the axis of linear polarization if there is such a nonzero component. The relative proportion of linear polarization we will term the *partial polarization* varying between 0 (completely unpolarized light) and 1 (completely linearly polarized light). Partial polarization is also known as the *degree of polarization* [8]. The orientation of linear polarization we will term the *phase* or simply the *orientation* of polarization. Note that the phase varies within the range 0–180°. Together the parameters i) intensity, ii) partial polarization, and, iii) phase, completely determine the state of partial linear polarization. A detailed definition of polarization is described in [8] and [3].

A state of partial linear polarization can be measured using a linear polarizing filter which resolves the electric field distribution of light along a given orientation. At a pixel in an image the transmitted intensity of partial linear polarized light through a linear polarizing filter varies sinusoidally with period 180° as a function of polarizer orientation. We term this the *transmitted radiance sinusoid*. The maximum, $I_{\max}$, of this sinusoid occurs when polarizer orientation is aligned parallel to the orientation of the linear polarized component, and the

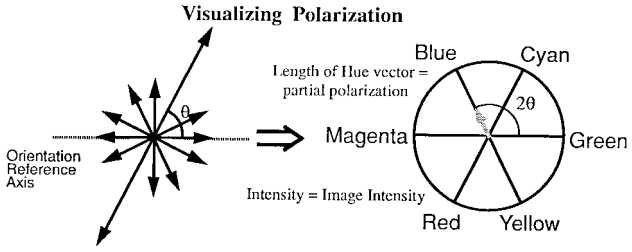

Fig. 2. Hue-saturation-intensity representation scheme for partial linear polarization.

minimum, $I_{\min}$, occurs when polarizer orientation is aligned perpendicular to the linear polarized component. With no linear polarized component the sinusoid is simply a horizontal line with one-half the intensity magnitude of the unpolarized light. With no unpolarized component the minimum value of the sinusoid is 0. Since a sinusoid can be uniquely determined by three points, three transmitted intensity measurements can be taken between 0 and 180° to uniquely determine partial linear polarization. We have standardly taken measurements at 0, 45, and 90°. Representing the image intensities obtained at each pixel by I_0, I_{45}, I_{90}, respectively, if θ represents where $I_{\min}$ occurs relative to the selected 0° orientation, then the three parameters for partial linear polarization can be derived from these image intensities according to

$$\text{(phase)} \qquad \theta = (1/2)\tan^{-1}\left(\frac{I_0 + I_{90} - 2I_{45}}{I_{90} - I_0}\right) \tag{1}$$

$$\text{if } (I_{90} < I_0) \text{ [if } (I_{45} < I_0)\ \theta = \theta + 90 \text{ else } \theta = \theta - 90]$$

$$\text{(intensity)} \qquad I_{\max} + I_{\min} = I_0 + I_{90} \tag{2}$$

$$\text{(partial polarization)} \qquad \frac{I_{\max} - I_{\min}}{I_{\max} + I_{\min}} = \frac{I_{90} - I_0}{(I_{90} + I_0)\cos 2\theta}. \tag{3}$$

Note that similar sets of equations can be derived for θ defined relative to any well-defined reference point on the transmitted radiance sinusoid (e.g., $I_{\max}$, inflection points, etc.). Regardless of what convention is used, θ is directly related to the orientation of the linearly polarized component, with respect to some offset.

Fig. 2 shows a mapping of the transmitted radiance sinusoid for partial linear polarization into a hue-saturation-intensity visualization scheme proposed in [28] and [26]. For a precise definition of the hue-saturation-intensity color space see [9]. Phase and partial polarization which are not observed by human vision are represented respectively in terms of hue and saturation. Since phase of polarization is in the range 0–180°, phase angle is multiplied by two to utilize the complete range of hue representation. Chromaticity at a pixel in a polarization image means that there is some presence of linear polarization as saturation corresponds directly to partial polarization. Unpolarized light at a pixel in a polarization image is therefore achromatic. Intensity is of course simply intensity itself.

There are two physical principles of reflected polarization which are basic to Polarization Vision that are detailed in [25], [27]. The *plane of incidence* at an object point viewed by a camera sensor is determined by the surface normal at the point and the viewing direction with respect to the corresponding pixel element within the camera sensor.

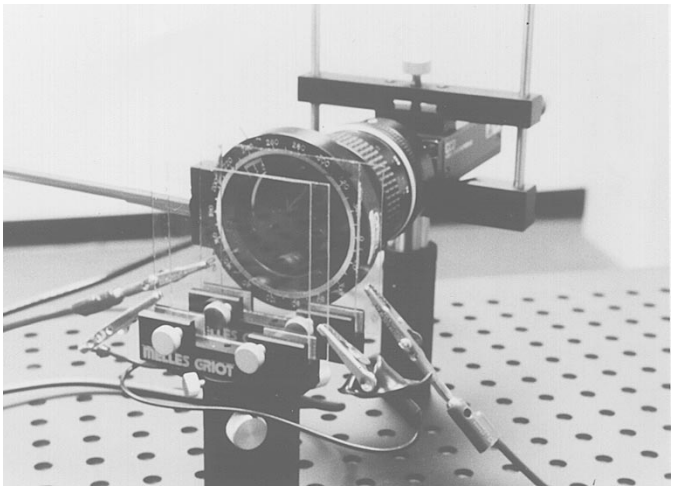

Fig. 3. Liquid crystal polarization camera.

- For unpolarized incident light, specular reflection (i.e., glossy reflection) has nonzero partial polarization, except for normal and grazing incidence, with linear polarized component oriented *perpendicular* to the plane of incidence.
- Diffuse reflection from dielectric surfaces for most viewing angles is essentially unpolarized, becoming significantly partial polarized at greater than 60° with respect to the angle between the viewing direction and the surface normal. The orientation of the linear polarized component is *parallel* to the plane of incidence for diffuse reflection. For smooth dielectric surfaces this is true for any incident polarization state.

In the domain of intensity vision there has been much research in the detection of specular reflection (e.g., [19], [6]) and using specular reflection to infer shape information (e.g., [14], [2], [5]).

Another important mode of physical information for interpreting objects in a scene is identification of intrinsic material classification. The capability of determining whether parts of an object are metal (conductor) or dielectric (nonconductor) can be very useful to object recognition and material inspection in manufacturing (e.g., circuit board inspection, package inspection, etc.). Healey [12], [11], proposed color based methods for dielectric/metal material classification. More recently polarization cues were discovered that can locally determine relative electrical conductivity of materials, with metal and dielectric at the extremes. The theory of this is explained in [24] and [25]. It turns out that if the specular angle of incidence is between 30° and 80°, and the specular component of reflection is strong relative to the diffuse component, the quantity

$$\frac{I_{\max}}{I_{\min}} \tag{4}$$

derived from transmitted radiance sinusoid parameters, is a very reliable discriminator for varying levels of electrical

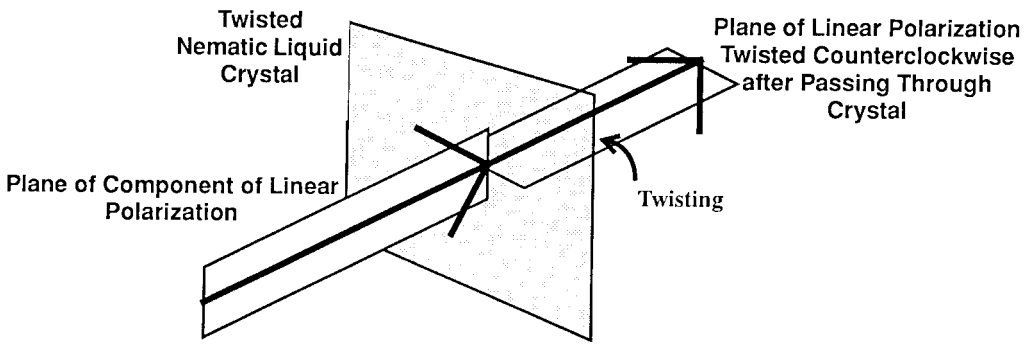

Fig. 4. Rotation of the linear polarized component of partially linear polarized light by a twisted nematic liquid crystal.

conductivity. This ratio for most metals varies between 1.0 and 2.0 while for dielectrics this ratio is above 3.0.

The section on Experimental Results shows how our fully automatic liquid crystal polarization camera, empirically demonstrates some of these principles.

III. Theory of Operation of a Liquid Crystal Polarization Camera

Obtaining the transmitted radiance sinusoid by rotating a polarizing filter in front of a CCD camera is a mechanically active process that produces optical distortion and is difficult to fully automate. Unless the axis perpendicular to the polarizing filter is exactly aligned with the optic axis of the camera, small shifts in projection of world points onto the image plane occur between different orientations of the polarizing filter. At intensity discontiniuites in a scene, significant shifts in image intensity are observed giving the false interpretation of reflected partial polarization even if it does not exist. Fully automating the mechanical rotation of a polarizing filter would require a motor that would have to precisely rotate the filter in synchronization with video frame rates.

Fig. 3 shows the liquid crystal polarization camera with a fixed polarizer and two twisted nematic liquid crystals mounted in front of an intensity CCD camera. Nothing mechanically rotates; the polarizer remains fixed while the twisted nematic (TN) liquid crystals electrooptically rotate the orientation of the linearly polarized component of reflected partial linear polarized light. The unpolarized component is not effected. In general the transmitted radiance sinusoid can be recovered by the *relative* rotation of the plane of linear polarization with respect to the polarizer. Each TN liquid crystal is binary in that it either rotates the plane of linear polarization by fixed n degrees, $0° < n \leq 90°$, which is determined upon fabrication, and 0 degrees (i.e., no twist). We use two TN liquid crystals, one at $n = 45°$, and the other at $n = 90°$, to insure at least three samplings of the transmitted radiance sinusoid. By electrically switching the states of two TN liquid crystals in front of a fixed linear polarizer, in synchronization with an intensity CCD camera, measuring the components of polarization of reflected light from objects can be placed under full computer control.

Liquid crystals come in different varieties and some of the theory behind them can be quite involved [21]. The molecular structure of the material in *twisted nematic* liquid crystals is helical, twisting slowly from one face of the crystal to the other face by a predesigned fixed amount n degrees. With no voltage applied across the liquid crystal faces, the plane of linear polarized light rotates along the helix by n degrees. See Fig. 4. When an ac voltage is applied across the liquid crystal faces, the helices straighten out so that the plane of linear polarized light is not rotated in this state. The switching or "relaxation" time of TN liquid crystals is now on the order of 1/30 of a second (i.e., one video frametime). This is much faster than the TN liquid crystals originally used in [28] which had a switching time of 1/10 of a second. The switching of TN liquid crystal states leaves the geometry of the optical projection of the world scene onto the image plane virtually unchanged. Another very nice property is that the polarizing properties of TN liquid crystals are fairly constant across a $\pm 30°$ conical field of view relative to the normal to the face of the crystal.

A complete layout of the liquid crystal polarization camera is shown in Fig. 5. The driver for the liquid crystals modulates a high frequency ac voltage so as to produce up to 4 states between the two TN liquid crystals, 0, 45, 90, and 135°. The driver also provides synchronization which, i) insures that an image from the CCD camera is digitized when the TN liquid crystal is in a fully relaxed state, and ii) insures that the state (i.e., the "twist") of both the TN liquid crystals are known with respect to each digitized image. Each state lasts two frametimes ($2 \times 1/30 = 1/15$ seconds) in which the liquid crystals are allowed to switch in the first frametime, and an image is digitized and stored during the second frametime. From the discussion in Section II about partial linear polarization, only three of the liquid crystal states are required to respectively produce three polarization component images sensed in sequence to measure partial linear polarization at each pixel. The timing scheme for the Liquid Crystal Polarization Camera shown in Fig. 5 utilizes only the 0°, 45°, and 90° states of the TN liquid crystals. During the one frametime it takes the liquid crystals to relax between each state, the most recent set of three polarization component images are processed to produce the hue-saturation-intensity visualization scheme for partial linear polarization shown in Fig. 2. The phase, intensity, and partial polarization at each pixel are respectively computed from expressions 1, 2, and 3 which are implemented using look-up tables on the Datacube MV-20. While partial linear polarization images are updated 15 times per second, each element of a scene must remain static over a period of 6 frametimes over which to obtain

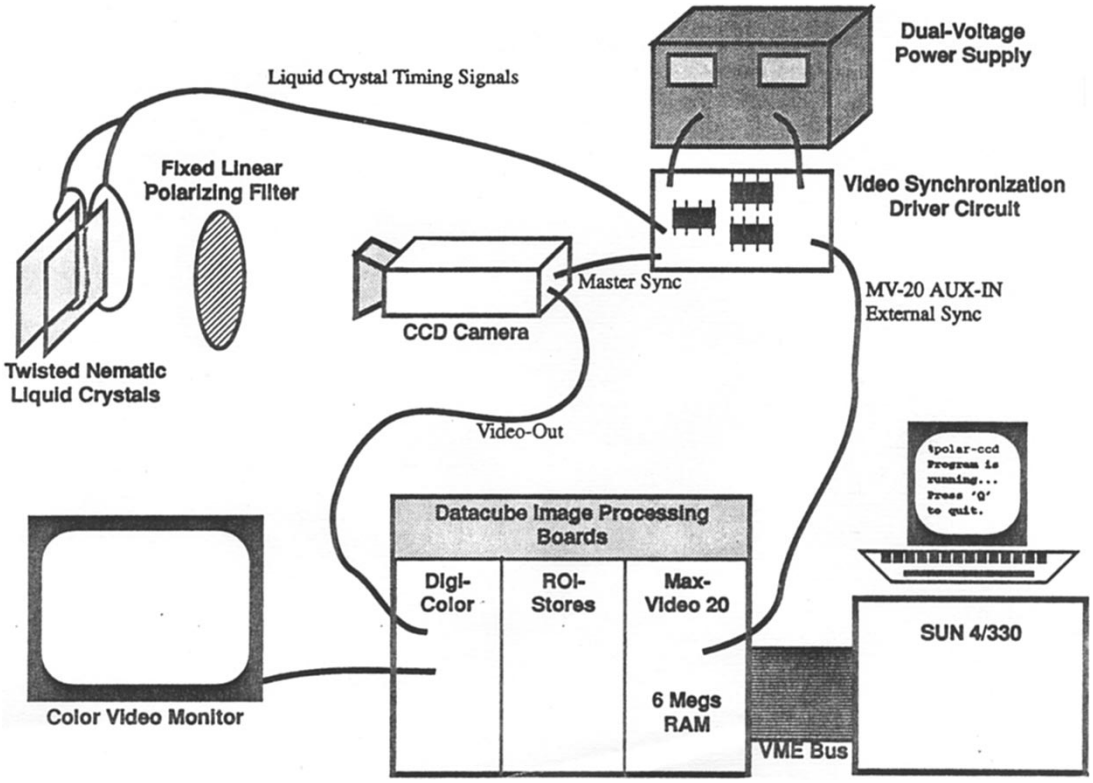

Fig. 5. Complete schematic diagram of the liquid crystal polarization camera interfaced with digital hardware.

all three polarization component images making the effective polarization imaging rate at $30/6 = 5$ Hz.

IV. Experimental Results

Fig. 6(a) shows a partial linear polarization image of a radial polarization filter taken with our liquid crystal polarization camera. The filter is mounted in a ring and backlighted by a white poster board placed behind the filter. The poster board is uniformly illuminated by a single distant nearly point light source. In a radial polarization filter the transmission lines are concentric circles about the center as shown in Fig. 6(b). The orientation of linear polarization transmitted through a portion of the filter is parallel to the tangent of the circle going through that portion. This creates a pattern of linear polarization phases across a radial polarization filter much like a hue color wheel—the phases are equal going radially outward from the center with orientation of the polar angle about the center. Note in Fig. 6(a) that since the orientation range of polarization phase is 180° the range of the hue color wheel is spanned twice in going full circle around the filter. A radial polarization filter provides a very nice ground truth for determining how accurate our polarization camera measures the orientation angle (i.e., phase) of polarization. We used an Oriel model 25328 radial polarization filter. By fitting a circle to the outer edge of the imaged radial polarization filter, its image radius and center were computed enabling us to know what angle the phase of polarization should be at each point on the filter. This was compared with the phase of polarization measured by our polarization camera. On average the phase of polarization was accurate to $\pm$ 0.85° for various polarization images taken at different light levels from bright to dark (i.e., from grey levels 240 down to 50, image intensity was nearly constant across the radial polarization filter in each image). Therefore, over an orientation range of 180°, the measurement of polarization phase by our camera has a signal-to-noise ratio of significantly over 100-to-1 under these conditions.

Measured partial polarization across the radial polarization filter varied between 0.99 and 1.0 regardless of phase of polarization and light level. The linear polarizing efficiency across the radial polarization filter we used is rated at better than 99%, and our measurement of partial polarization is consistent with this. For polarization images of the radial polarization filter, and a regular linear polarizing filter also rated at better than 99% linear polarizing efficiency, partial polarization was consistently measured to be between 0.99 and 1.0 across these filters suggesting a partial polarization accuracy of well within 0.01 out of 1.0 for these images. We passed light through an Oriel frosted glass plate producing a uniform field of unpolarized light and our polarization camera measured partial polarization varying between 0.0 and just above 0.01. For measured intensity we observed the standard deviation of grey value intensities taken with our polarization camera over various images to be within ± 3 as compared with the the standard deviation of grey value intensities from each of the CCD cameras to be about ± 2. Measurement of polarization phase from the radial polarization filter started to seriously degrade when transmitted intensity level went below grey value 20.

In comparison we took similar measurements utilizing a mechanically rotating polarizer without the use of the liquid crystals. For the radial polarization filter we observed an average phase of polarization accuracy of just within $\pm 3°$.

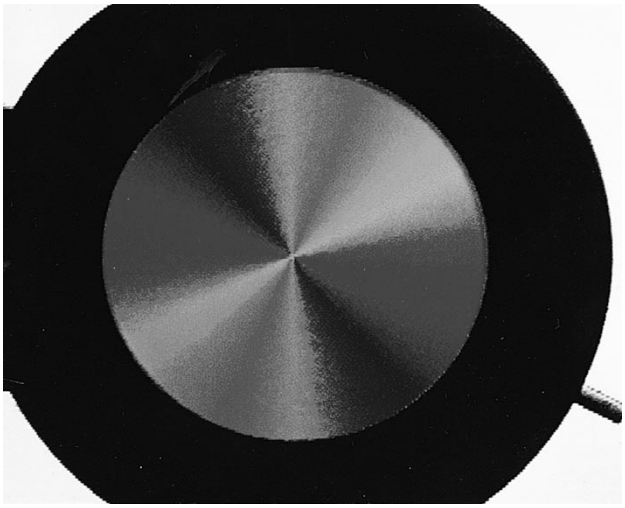

(a)

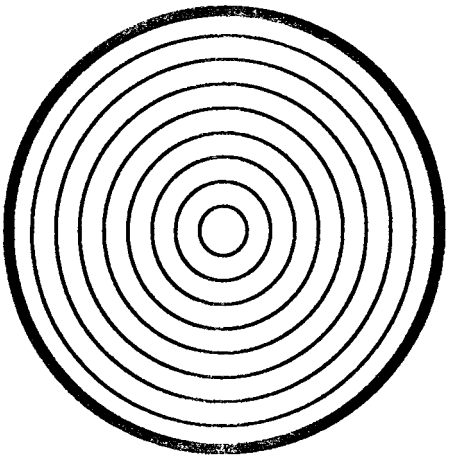

(b)

Fig. 6. (a) Polarization image of a radial polarization filter taken with the liquid crystal polarization camera. (b) Diagram depicting concentric circles of linear polarizing transmission orientations in a radial polarization filter. At a point on a radial polarizing filter, light becomes linearly polarized at an orientation that is tangent to the circle going through that point.

The accuracy of phase measurement increased the further away from the center of the radial polarizer, and got worse near the center. This is consistent with the fact that phase of linear polarization spatially varies more rapidly nearer the center of the radial polarizer and that the mechanical rotation of the linear polarizer produces a fixed translational shifting across the image. The measurement of partial polarization varied between 0.98 and 1.0 across the radial polarizer, just a little worse than when using the liquid crystals. However, this was for a uniformly back illuminated filter. As comparison between Fig. 7(b) and (c) below will attest, very large errors in polarization measurement occur when using a mechanically rotating polarizer at portions of scenes where there is significant local variation in intensity due to shading or edges.

Fig. 7(a) and (b) shows how polarization provides important information about a scene that would be very difficult and perhaps impossible to deduce from an intensity image. Fig. 7(a) shows the intensity image of what apparently are two mugs in a scene. Looking closely at the intensity image reveals that there is some difference between the two mugs; the left mug has its letters reversed. The only visual cues telling that the left mug is simply a reflection are very high level features such as the reversal of recognizable high level features (e.g., alphabet

(a)

(b)

(c)

Fig. 7. (a) Intensity image of a ceramic cup and its reflection in a glass mirror. (b) Partial linear polarization image produced from the liquid crystal polarization camera in Fig. 3 (at 5 Hz). (c) Partial linear polarization image produced from mechanically rotating a linear polarizing filter.

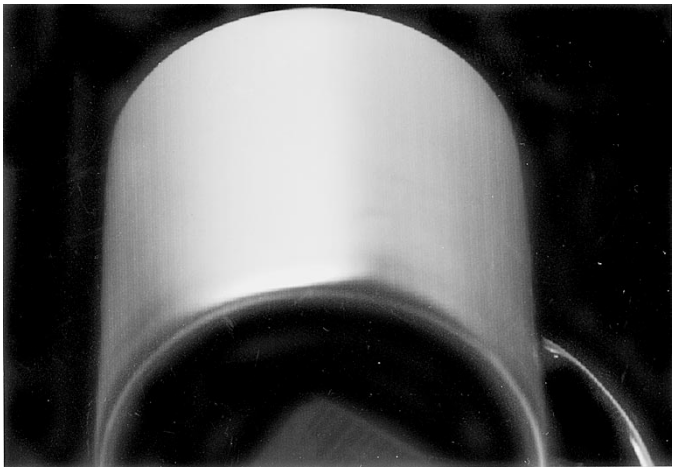

(a)

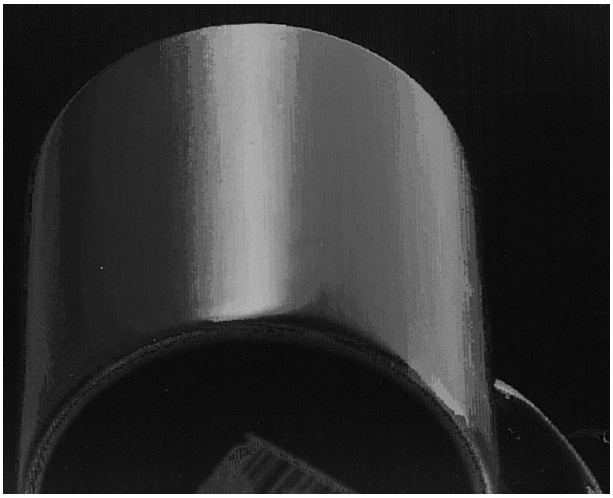

(b)

Fig. 8. (a) Intensity image of a cylindrical ceramic cup under extended illumination. (b) Partial linear polarization image of the cylindrical ceramic cup produced from the liquid crystal polarization camera.

letters) or the edge of the glass mirror. Otherwise the reflected intensity (and color) of the two mugs look essentially the same. This type of problem occurs in vision fairly frequently such as when stray specular glare from objects give the false interpretation that real edges actually exist there. Consider the problem of an autonomous land vehicle viewing a scene part of which is reflected by a lake or river. How does the vehicle know which are the "real" elements of the scene? How does a mobile robot know when it is running into a glass door, or if navigating according to edge cues, which are geometric edge cues opposed to specular edge cues? Fig. 7(b) was obtained with our liquid crystal polarization camera showing that the left mug has Cyan chromaticity implying significant partial polarization. Cyan chromaticity is also observed at specular highlights on the right mug as well. (The very bright center of specularities saturate the camera so that pixels record gray level 255 regardless of the state of the TN liquid crystals. This gives a flat transmitted radiance sinusoid, and hence, the appearance of unpolarized light, when in fact the reflected light from these areas are significantly partially polarized. This is a limitation of the dynamic range of the SONY XC-77

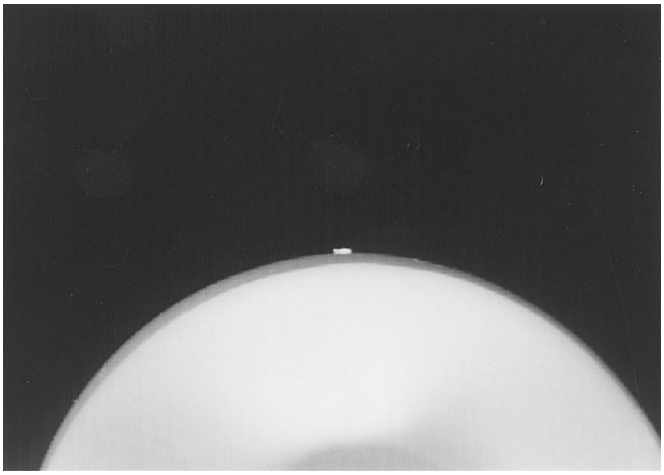

(a)

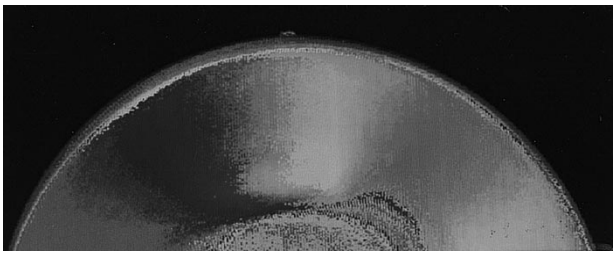

(b)

Fig. 9. (a) Intensity image of a spherical hemisphere of plastic under extended illumination. (b) Partial linear polarization image of the spherical hemisphere produced from the liquid crystal polarization camera.

CCD camera being used, and NOT our polarization vision algorithm.) Significant partial polarization is also observed at the occluding contour of the right mug as Red color. Note that the hue colors Cyan and Red are complementary colors indicative of transmitted radiance sinusoids 90° out of phase.

The scene in Fig. 7(a) is illuminated by two nearly point incandescent light sources, one source incident from just slightly oblique to the viewing direction, the other source from the back of the right cup. When taking the partial linear polarization image Fig. 7(b), the fixed polarizer analyzer on our liquid crystal polarization camera is oriented so that the transmission axis is horizontal. The hue Cyan represents when the plane of the linear polarized component of reflected light is vertical with respect to the image (i.e., when the transmitted radiance sinusoid is observed minimum when both TN liquid crystals are in the zero twist "ON" state). Using the itemized physical principles discussed in Section II, Cyan hue corresponds to specular reflection when the plane of incidence is horizontal relative to the image. As it turns out the planes of incidence in this scene are all approximately horizontal. The Red color hue representing a 90° transmitted radiance sinusoid phase difference relative to the Cyan color hue is indicative of partial polarization from diffuse reflection near an occluding contour. Note the thin edge of specular reflection occurring at the very edge of the occluding contour on the right mug. Even when the planes of incidence are not known it is possible from polarization images to deduce which are the specular reflections and which are the occluding contours, from a number of physical principles [25], [27].

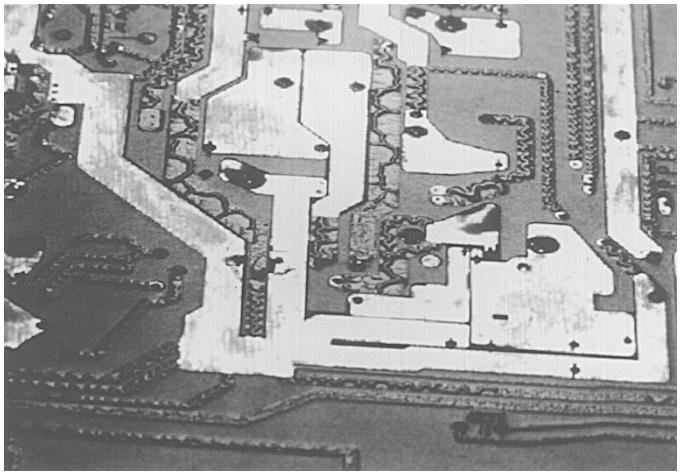

(a)

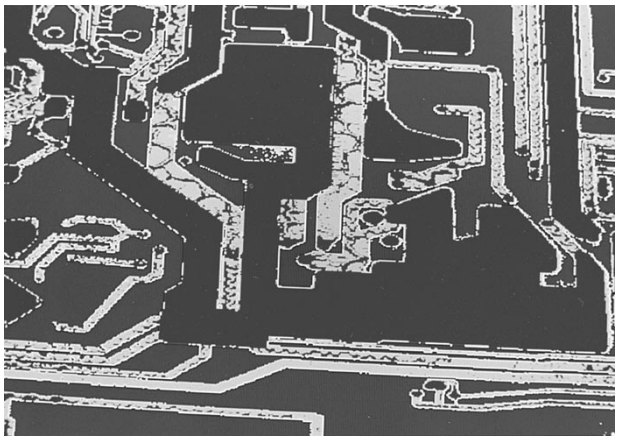

(b)

Fig. 10. (a) Intensity image of a circuit board with metal solder, plastic dielectric substrate, and translucent dielectric coating solder metal. (b) Material segmentation produced from liquid crystal polarization camera. Blue is dielectric, red is metal, yellow is translucent dielectric coating on solder metal. Some ted shows where translucent dielectric coating on solder is crinkled.

Fig. 7(c) shows the partial linear polarization image similar to Fig. 7(b) except with the use of mechanically rotating a linear polarizing filter without the liquid crystals. Note the false partial polarization effects around intensity edges due to the slight relative geometric shifting of the polarization component images for different rotational positions of the polarizing filter. Also observe how the measurement of the phase of partial linear polarization is effected at object points where there are shading variations in diffuse and specular reflection. This illustrates the significant improvement in the quality of obtaining partial linear polarization images by using the liquid crystals.

Fig. 8(a) and (b) shows, respectively, the intensity and polarization images of a cylindrical cup illuminated with an extended light source (a large area photography light tent) so as to produce specular reflection from a number of different surface orientations. The different color hues shown in the polarization image correspond to plane of incidence constraints containing the surface normal. In this example, Cyan color hue corresponds to planes of incidence oriented vertically in the image while the complementary color hue, Red, corresponds to planes of incidence oriented horizontal in the image. Almost the entire spectrum of color hues is displayed here. Fig. 9(a) and (b), respectively, shows the intensity and polarization images of one hemisphere of a plastic sphere illuminated with an extended light source. While the polarization image does not give completely unique surface orientation information, the pattern of plane of incidence constraints gives enough rudimentary shape information to distinguish different shape classes for object recognition. For instance, on a cylindrical shape the lines of constant color hue are parallel to one another while on a spherical shape lines of constant color hue mutually intersect at a point. Besides being useful in sorting-by-shape systems in manufacturing, outdoor objects illuminated by skylight serving as an extended illuminator may be able to be distinguished by shape class as well.

Fig. 10(a) shows a circuit board which has three basic types of material regions, i) solder metal, ii) plastic dielectric, and iii) solder metal coated with translucent plastic dielectric. The circuit board is illuminated with standard fluorescent ceiling lighting. Fig. 10(b) shows a material classification image. Fig. 10(b) shows in blue, yellow and red, a thresholding of the ratio $I_{\max}/I_{\min}$ greater than 3.0, between 2.0 and 3.0, and between 1.0 and 2.0, respectively. Blue physically corresponds to plastic dielectric, Yellow physically corresponds to solder metal coated with translucent dielectric, and Red physically corresponds to bare solder metal (see [24], [27] for theoretical details). Some of the translucent dielectric coating on the solder is "crinkled" and at these points $I_{\max}/I_{\min}$ is underestimated therefore producing a Red label. A method for determining when the dielectric coating is not smoothly deposited on the metal can be developed from this. This illustrates how physical information in a scene directly related to reflected polarization can be visualized by a polarization camera. Note that this technique works despite nonuniform lighting conditions. Intensity thresholding of Fig. 10(a) will not work as there are portions of the image where metal is darker than dielectric at other portions and vice versa. The potential application to manufacturing and quality control of circuit boards is clear. This can also be applied to object recognition whereby shape descriptions are augmented by description of material composition, in scenes where there is significantly extended specular reflection.

V. Conclusion

We presented the design and a particular implementation of a camera sensor that is geared to do polarization vision. This type of camera sensor, which we term a "polarization camera," subsumes the capabilities of existing intensity cameras in its ability to fully automatically resolve polarization components and output a polarization image which generalizes the information content of a standard intensity image. We exploited the principles of liquid crystal technology to fully automate the process of resolving polarization components, and presented a visualization scheme for mapping states of partial linear polarization into hue-saturation-intensity color space. Datacube boards digitize polarization component images and process these images to produce a partial linear polarization image. Experimentation with our liquid crystal polarization camera demonstrated some of its capabilities with respect to segmentation of specular reflection and occluding contours, obtaining shape constraints, and material

classification. Improvement of polarization image quality produced using liquid crystals was demonstrated over that produced from mechanical rotation of a linear polarizing filter. We can improve the dynamic range of the liquid crystal polarization camera by taking multiple sets of three polarization component images each set at a different F-stop setting which would ameliorate saturation problems such as the specularities in Fig. 7(a)—in this way the transmitted radiance sinusoid can be derived over a larger range of gray values.

The design of our liquid crystal polarization camera lays the groundwork for faster and more self-contained polarization camera designs. Liquid crystals are low cost and convenient to use, so they provide an elegant way of quickly converting a standard intensity CCD camera into a fully automatic partial linear polarization camera. We are in the process of modularizing the TN liquid crystals and polarizer into an optical head, and designing an electronic driver box to be compatible with virtually any NTSC video device, including portable handheld video cameras which will enable the exploration of the application potential of liquid crystal polarization cameras outside the laboratory.

REFERENCES

[1] G. D. Bernard and R. Wehner, "Functional similarities between polarization vision and color vision," *Vision Res.*, vol. 17, pp. 1019–1028, 1977.

[2] A. Blake, "Specular stereo," in *Proc. IJCAI*, 1985, pp. 973–976.

[3] M. Born and E. Wolf, *Principles of Optics*. New York: Pergamon, 1959.

[4] T. E. Boult and L. B. Wolff, "Physically-based edge labeling," in *Proc. IEEE Conf. Computer Vision and Pattern Recognition (CVPR)*, Maui, HI, June 1991.

[5] G. J. Brelstaff, "Inferring surface shape from specular reflections," Ph.D. dissertation, Dep. Comput. Sci., Univ. Edinburgh, 1989.

[6] G. J. Brelstaff and A. Blake, "Detecting specular reflections using Lambertian constraints," in *Proc. IEEE Second Int. Conf. Comput. Vision (ICCV)*, Tampa, FL, Dec. 1988, pp. 297–302.

[7] D. A. Cameron and E. N. Pugh, "Double cones as a basis for a new type of polarization vision in vertebrates," *Nature*, vol. 353, pp. 161–164, Sept. 1991.

[8] D. Clarke and J. F. Grainger, *Polarized Light and Optical Measurement* New York: Pergamon, 1971.

[9] J. D. Foley, A. van Dam, S. K. Feiner, J. F. Hughes, and R. L. Phillips, *Introduction to Computer Graphics*. Reading, MA: Addison-Wesley, 1994.

[10] C. W. Hawryshyn, "Polarization vision in fish," *Amer. Scientist*, vol. 80, pp. 164–175, Mar.–Apr. 1992.

[11] G. Healey, "Using color for geometry-insensitive segmentation," *J. Opt. Soc. Amer. A*, vol. 6, no. 6, pp. 920–937, June 1989.

[12] G. Healey and T. O. Binford, "Predicting material classes," in *Proc. DARPA Image Understanding Workshop*, Cambridge, MA, Apr. 1988, pp. 1140–1146.

[13] B. K. P. Horn and R. W. Sjoberg, "Calculating the reflectance map," *Appl. Opt.*, vol. 18, no. 11, pp. 1770–1779, June 1979.

[14] K. Ikeuchi, "Determining surface orientations of specular surfaces by using the photometric stereo method," *IEEE Trans. Pattern Anal. Machine Intell.*, vol. 3, pp. 661–669, Nov. 1981.

[15] B. F. Jones and P. T. Fairney, "Recognition of shiny dielectric objects by analyzing the polarization of reflected light," *Image and Vision Comput. J.*, vol. 7, no. 4, pp. 253–258, 1989.

[16] K. Koshikawa and Y. Shirai, "A model-based recognition of glossy objects using their polarimetric properties," *Advances in Robotics*, vol. 2, no. 2, 1987.

[17] G. A. Mazokhin-Porshnyakov, *Insect Vision*. New York: Plenum, 1969.

[18] S. Rossel and R. Wehner, "Polarization vision in bees," *Nature*, vol. 323, pp. 128–131, Sept. 1969.

[19] S. Shafer, "Using color to separate reflection components," *Color Res. Applicat.*, vol. 10, pp. 210–218, 1985.

[20] T. H. Waterman, "Polarization sensitivity," *Handbook of Sensory Physiology, Vision of Invertebrates*, H. J. Altrum, Ed. New York: Springer Verlag, 1981, vol. 7, part 6b, pp. 283–463.

[21] E. B. Priestly, P. J. Wojtowicz, and P. Sheng, *Introduction to Liquid Crystals*. New York: Plenum, 1975.

[22] L. B. Wolff, "Surface orientation from polarization images," *Proc. Opt., Illumin. Image Sensing for Machine Vision II*, SPIE, Cambridge, MA, vol. 850, pp. 110–121, Nov. 1987.

[23] ———, "Using polarization to separate reflection components," in *Proc. IEEE Conf. Comput. Vision and Pattern Recognition (CVPR)*, San Diego, CA, June 1989, pp. 363–369.

[24] ———, "Polarization-based material classification from specular reflection," *IEEE Trans. Pattern Anal. Machine Intell.*, vol. 12, pp. 1059–1071, Nov. 1990.

[25] ———, "Polarization methods in computer vision," Ph.D. dissertation, Columbia Univ., NT, Jan. 1991.

[26] ———, "Polarization camera technology," in *Proc. DARPA Image Understanding Workshop*, Washington, D.C., Apr. 1993, pp. 1031–1036.

[27] L. B. Wolff and T. E. Boult, "Constraining object features using a polarization reflectance model," *IEEE Trans. Pattern Anal. Machine Intell.*, vol. 13, pp. 635–657, July 1991.

[28] L. B. Wolff and T. A. Mancini, "Liquid crystal polarization camera," in *Proc. IEEE Workshop Applicat. Comput. Vision*, Palm Springs, CA, Dec. 1992, pp. 120–127.

Lawrence B. Wolff received the B.S. degree in mathematics and physics from Yale University, New Haven, CT, in 1981, and the M.S. and Ph.D. degrees in computer science from Columbia University, New York, NY, in 1988 and 1991 respectively.

He is an Associate Professor of computer science at The Johns Hopkins University, Baltimore, MD, where he directs the Computer Vision Laboratory. His interests are in computer vision, sensors for robotics and vision, computer graphics, and differential geometry. He is a co-editor of the three volume book series *Physics-Based Vision: Principles and Practice* (1992).

Dr. Wolff received an NSF National Young Investigator award in 1993 for his research in polarization vision.

Todd A. Mancini received the B.S. and M.S. degrees in computer science in 1991 and 1993, respectively, from The Johns Hopkins University, Baltimore, MD.

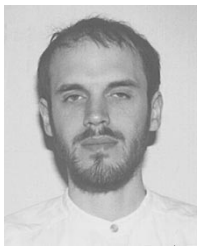

Phillippe Pouliquen is a Ph.D. student with the Department of Electrical and Computer Engineering at The Johns Hopkins University, Baltimore, MD.

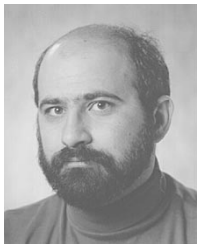

Andreas G. Andreou is an Associate Professor with the Department of Electrical and Computer Engineering at The Johns Hopkins University, Baltimore, MD.